Geofísica Internacional (2011) 50-3: 319-340

Original paper

New locations of volcano-tectonic earthquakes under Popocatépetl Volcano applying a Genetic Search Algorithm

Pia Berger*, F. Alejandro Nava Pichardo, Carlos Valdés González and Alicia Martínez Bringas

Received: August 27, 2010; accepted: December 8, 2010; published on line: June 30, 2011

Resumen

En los inicios de los años noventa, después de ~70 años de quietud, la actividad sísmica bajo el Volcán Popocatépetl en el centro de México se reactivo, comenzando un período de alta actividad volcánica. Esta actividad continúa hasta la fecha y ha provocado emisiones importantes de gases volcánicos, así como formación de domos y erupciones moderadas. Hemos aplicado un algoritmo genético de búsqueda, para ajustar las diferencias de los tiempos de arribo de cada sismo individualmente, para obtener relocalizaciones de alta precisión (~200 m) para 405 sismos volcano-tectónicos (VT) de un grupo inicial de 968 eventos registrados por una red local de 1995 a 2006. Comparamos los resultados de la relocalización con los obtenidos aplicando el método de dobles diferencias. El objetivo de este trabajo es el de caracterizar la sismicidad, determinar parametros hipocentrales y explorar fuentes sísmicas.

Los resultados del presente análisis mejoran la determinación de la distribución de la actividad sísmica, permitiendo observar características que ocultaba la dispersión en las localizaciones. La agrupación difusa de eventos, asociada con una falla previamente identificada en el SE, aparece ahora como un sistema de fallas que consiste de al menos una falla con rumbo NW-SE, atravesada por otra falla con rumbo NE-SW.

Se encontró que la ocurrencia de sismos ha variado localmente con el tiempo. Algunas alineaciones de eventos coinciden con fallas previamente identificadas. Otras agrupaciones lineales de eventos sugieren fallas ocultas reactivadas por actividad volcánica, como intrusiones de diques, o degasificación de un cuerpo magmático bajo el Volcán Popocatépetl.

Palabras clave: Volcán Popocatépetl, relocalización, algoritmos genéticos de diferencias de tiempos de arribo, doble diferencia.

Abstract

In the early 1990's, after ~70 years of quiescence, seismic activity was renewed beneath Popocatépetl Volcano, central Mexico, and a period of high volcanic activity began. This activity continues today, and has featured high emissions of volcanic gases and fumaroles, dome filling processes, and moderate eruptions. The three largest explosive eruptions occurred in 1997, 2001, and 2003.

We applied a genetic search algorithm to fit arrival-time differences on an individual basis, and we obtain high precision (~200 m) relocations for 405 volcano-tectonic (VT) events from 968 events recorded by a local network from 1995 to 2006. We compare these results to relocations obtained by applying a double-difference algorithm. The objective is to characterize the seismicity, determine hypocentral parameters, and explore seismic sources.

The results shed light on the distribution of seismic activity, revealing features previously hidden by location scatter. A diffuse cluster associated with a previously-identified SE-trending fault now appears to be associated with a fault system consisting of at least one NW-SE trending fault crossed by a NE-SW trending fault.

Event occurrence was found to be locally time-dependent. Some aligned events coincide with previously-proposed faults. Other linear clusters may indicate hidden faults being activated by volcanic activity, such as dike intrusion or degassing of the magma body below Popocatépetl Volcano.

Key words: Popocatépetl Volcano, relocalization, arrival-time difference genetic algorithm, double-difference.

P. Berger*
Instituto de Geofísica
Departamento de Sismología
Universidad Nacional Autónoma de México
Ciudad Universitaria
Delegación Coyoacán, 04510
México D.F., México
*Corresponding author: piaahoi@gmail.com

F. A. Nava Pichardo
Centro de Investigacion Científica
y Educacion Superior de Ensenada
22860, BC, Mexico

C. Valdés González
Instituto de Geofísica
Departamento de Sismología
Universidad Nacional Autónoma de México
Ciudad Universitaria
Delegación Coyoacán, 04510
México D.F., México

A. Martínez Bringas
Centro Nacional de Prevencion de Disastres
Delegación Coyoacán, 04510
México D.F., México

Introduction

Earthquake location is usually performed using hypocentral location algorithms, such as Hypo71 (Lee and Lahr, 1972), Hypoinverse (Klein, 1985), or Hypocenter (Lienert *et al*., 1986; Lienert, 1994). Those location algorithms are based on the pioneering work of Geiger (1910). The error between observed and calculated seismic phase arrival times is minimized in a least squares sense by linearization of the location problem through iteratively modifying hypocenter and origin times, in order to satisfy the given a *priori* information. These methods have various disadvantages, especially when optimal station coverage is lacking, when no S-wave arrival times are used, or when rough topography affects travel times. This is why a first instance earthquake location may be self-consistent, without necessarily being accurate (Lomnitz, 2006), and why relocation, which consists of a newly-performed location of already located events using more sophisticated methods, is important.

Accurate event location is important and necessary in order to understand the behavior and characteristics of active volcanoes like Popocatépetl. Whereas on a global scale earthquake location allows imaging of the major geodynamic features of the Earth, its accuracy remains too low to allow description of many seismo-tectonic features at local scales and in highly heterogeneous media such as volcanoes. At local scales, an unfavorable geometry of either the earthquake spatial distribution and/or the seismic network stations generates trade-offs between model parameters and induces uncertainties in earthquake locations. Double-difference relocation methods developed in the last decades (e.g., Jordan and Sverdrup, 1981; Poupinet *et al*., 1984; Ito, 1985; Got and Frechet, 1994; Slunga *et al*., 1995; Shearer, 1997; Rubin *et al*., 1998; Waldhauser and Ellsworth, 2000) have shown that knowledge about a seismogenic region may be significantly changed after accurate relocation of earthquakes (see Wolfe, 2002) for a discussion of double-difference algorithms). The limitations of these methods are not always taken into account, however, so that too large a confidence is sometimes placed on their results.

In this study, we apply both methods: (1) a common double-difference method and (2) a newly developed relocation method, which is based on a genetic algorithm, a global optimization search method.

Geological setting

Popocatépetl Volcano (5,452 m) is one of the most active stratovolcanoes in Mexico (Fig. 1), located in the central part of the Mexican Volcanic Belt, a volcanic arc related to the subduction of the oceanic Cocos and Rivera plates beneath the North American plate. Popocatépetl poses a major geological hazard for Mexico, as a sudden eruption could threaten highly populated areas, including Mexico City (60 km northwest of the crater) and Puebla (40 km east of the crater); in all, more than 10 million people are living within 70 km of the volcano (Siebe *et al*., 1996; De la Cruz-Reyna and Siebe, 1997; Macías and Siebe, 2005).

The current phase of seismic activity in Popocatépetl began in 1990 (De la Cruz-Reyna *et al*., 2008), with a large increase occurring in 1993 and explosive reactivation starting in December 1994, after nearly 70 years of dormancy (Siebe *et al*., 1996; De la Cruz-Reyna and Siebe, 1997). Since 1996, several dome emplacement-destruction processes have taken place (Arciniega Ceballos *et al*., 2000; Wright *et al*., 2002). Due to its high potential risk, many geological and geophysical studies have been carried out on the volcano (e.g., Valdés *et al*., 1995; Campillo *et al*., 1996; Shapiro *et al*., 1997; Espíndola *et al*., 2004; Espinasa-Perena and Martín Del Pozzo, 2006).

López Ramos (1983) proposes the existence of a basement of limestones and granodiorites beneath Popocatépetl volcano, extrapolating geologic data from the surrounding areas. Valdés González and Comité (1994) propose that regional basement structure occurs at a depth of 9 km b.s.l. (below sea level). Geological studies from e.g. Fries (1965), Meritano-Arenas *et al*. (1998) indicate that the volcano rests upon a stratum of limestone (-1.5 km b.s.l.) and metamorphic rock (~ sea level): limestones and metamorphic rocks are exposed as isolated outcrops related to horst and graben fault structures more than 20 km south of Popocatépetl's summit. Geophysical, geological and geochemical studies on Popocatépetl have led to controversial results, so that until now the crustal seismic structure beneath Popocatépetl is not well understood. Straub and Martín-Del Pozzo (2001) suggest that an andesitic magma rises from the moho and mixes with another dacitic melt at depths of ~4 to 13 km below the crater. Based on gravimetric measurements, Espíndola *et al*. (2004) modeled density difference below the volcano, and interpreted a 25 km^3 negative density contrast at a depth of 7 km b.s.l. as the magma chamber. Studies on fluid inclusions by Atlas *et al*. (2006) and Roberge *et al*. (2007) negate the existence of a large magma chamber at depths shallower than 4.5 km b.s.l. and propose a dike and sill system instead.

Popocatépetl is subjected to the regional stress state, which is SE-NW for the minimal stress σ_3,

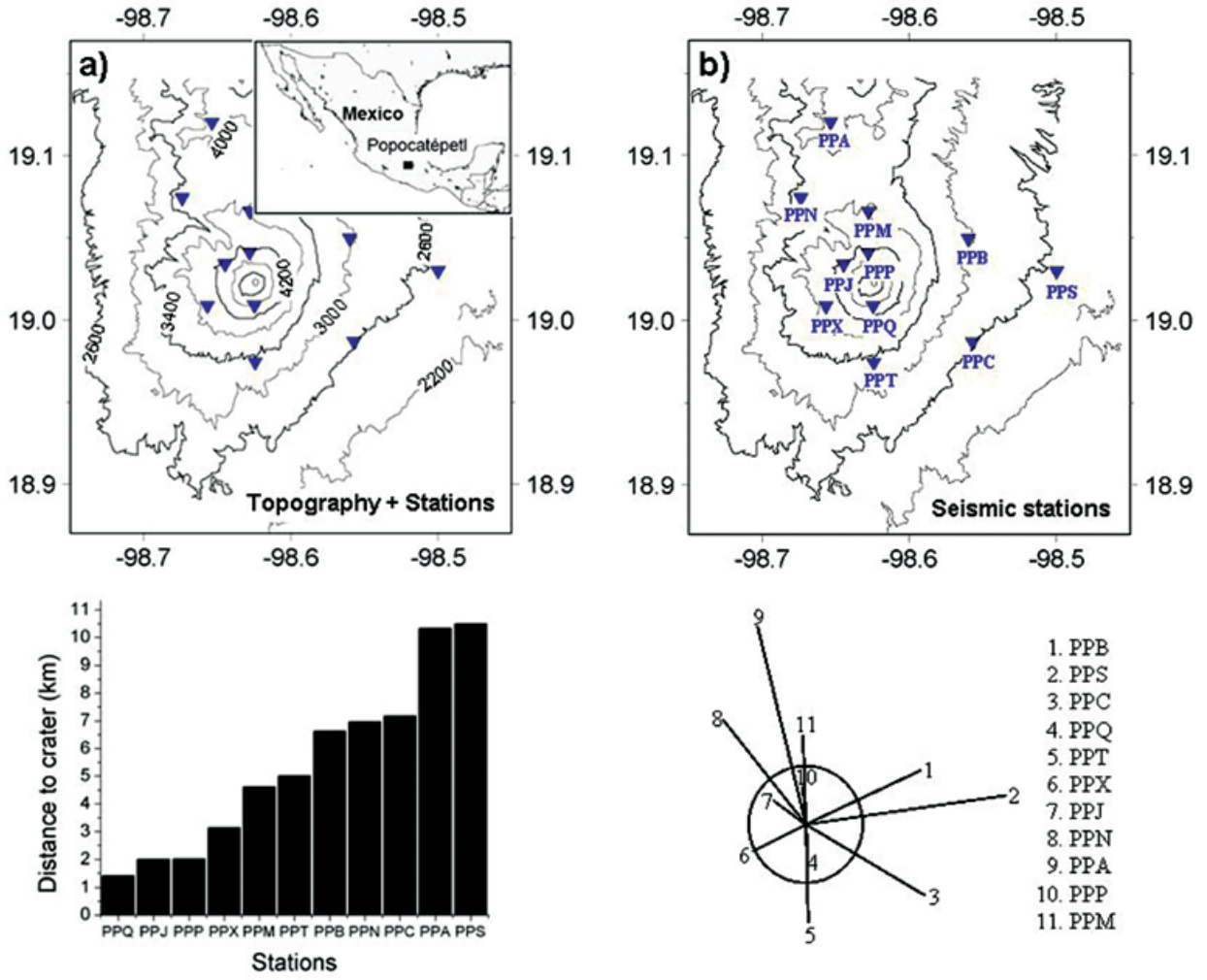

Figure 1. a) Location of Popocatépetl volcano, Mexico (inset), with contoured topography; triangles representing the seismic stations b) Seismic stations (solid triangles) installed between 1995 and 2006. c) Distance (km) of stations used in this study from the crater. d) Azimuthal station distribution with relative distances from the crater. Circle represents 3 km from the crater. 1. PPB (Bonsai), 2. PPS (Techalotepec), 3. PPC (Colibri), 4. PPQ (Los Cuervos), 5. PPT (Tetexcaloc), 6. PPX (Chipiquixtle), 7. PPJ (Juncos), 8. PPN (Lomo del Negro), 9. PPA (Alzomoni), 10. PPP (Canario), 11. PPM (Tlamacas).

SW-NE for the medium stress σ_2, and vertical for the principal stress σ_1 (Ego and Ansan, 2002; Arámbula-Mendoza *et al*., 2010). The study by Arámbula-Mendoza *et al*. (2010), who calculated the focal mechanisms of volcanic events, showed that magma movement and volcanic activity can locally influence these stress axes.

Seismic monitoring of recent activity at Popocatépetl

The volcano-tectonic activity of Popocatépetl began in 1990 (De la Cruz-Reyna *et al*., 2008), while its explosive reactivation started in December 1994. In 1995, seven seismic stations (PPM, PPC PPP, PPX, PPQ, PPS, PPB) from the National Seismological Service (SSN) were operating at distances between 1.5 and 10.5 km from the volcano (Fig. 1b, c, d). Through the efforts of the SSN and the National Center for Disaster Prevention, Mexico (CENAPRED), the seismograph network eventually grew to seven stations. The stations are sited on the volcano's flanks, at altitudes from 2500 to 4450 m. Five of the stations (PPM, PPC, PPX, PPQ, and PPP) are three-component seismometers, and two of them (PPS and PPB) are vertical-component only. All stations have 1 Hz natural frequency sensors. In the following years, the network expanded to include three triaxial stations of 1 Hz natural frequency: PPN (September 1995), PPT (May 1996), and PPJ (November 1997). In

March 1998, the network was augmented when the triaxial broadband station PPA was installed and the short period station PPP was upgraded to broadband. In July 1998, the array was completed with an upgrade of station PPX to broad-band capabilities. The Popocatépetl network, shown in Figure 1, operated continuously with 11 stations, until station PPB failed in June 1997, station PPN in November 1997, and station PPA in August 1998. Since 2000, the network has been operating with nine stations.

For the period from November 1995 to December 2006, about 1,800 identifiable volcano-tectonic (VT) earthquakes were recorded, with coda magnitudes ranging from M_C 1.17 to 3.80. VT earthquakes are indistinguishable from common double-couple tectonic earthquakes; they have been interpreted as the brittle response of volcanic rocks fracturing due to fluid pressure superimposed on the regional stress field (e.g., Chouet, 1996), and act as indicators of stress concentrations within the area surrounding magma reservoirs and conduits. Because they originate as abrupt shear motion along faults, the seismograms of VT-events typically show an impulsive onset followed by coda waves, whose spectral peaks are broadly distributed between 3 and 18 Hz.

Waveform data from the Popocatépetl network were telemetered to CENAPRED, and a central GPS-clock was used to control time for the detection system. First-arrival times on the seismograms from VT earthquakes were manually identified, and earthquake locations were determined using the Hypocenter earthquake location algorithm (Lienert and Havskov, 1995; Havskov, 2003); and the 1-D layered P-wave velocity model from Valdes-González and Comité (1994) (Line 3 blue, dash-dotted, Fig. 4). The description of this and other velocity models is given in section 4. Initially, several velocity models were tested for the location of the largest VT-earthquakes, which had clear arrivals and were detected by most of the stations. The model which produced the smallest arrival-time residuals with Hypocenter was the one proposed by Valdes-González and Comité (1994), which resulted in an average root mean square (RMS) residual of 0.12 sec for about 800 located VT events. The maximum adjusted location error was calculated to be 0.25 km, as an average of the horizontal and vertical errors reported by Hypocenter.

Velocity models

For our study, preliminary locations (see § 5.1) were obtained using the single event program Hypocenter (Lienert and Havskov, 1995) and the Valdés-González and Comité (1994) 1-D velocity model.

The model from Valdés-González and Comité (1994) and two other velocity models from Cruz-Atienza *et al*. (2001) and De Barros *et al*. (2008), all proposed for Popocatépetl volcano, were used to relocate our data set, using the genetic algorithm program (§ 5.2) and the double-difference algorithm (§ 5.3).

The shear wave velocity model from Cruz-Atienza *et al*. (2001) was obtained by inversion of receiver functions using four teleseismic events from South America at station PPIG (PPM), located 4 km north of the Popocatépetl crater; this model includes a low velocity zone between 6 and 10 km depth (3-7 km b.s.l.) (Fig. 4).

The model from De Barros *et al*. (2008) was obtained from analysis of Rayleigh waves and a recalculation of the phase velocities corresponding to several previous models. The shear-wave velocities in this model are similar to the MVB crust, and are close to those of the Valdés *et al*. (1986) model, which is based on a seismic refraction study in Oaxaca (Line 5, Fig. 4). P-wave velocity models were estimated from S-wave velocities models and vice versa, using a Poisson ration of Vp/Vs = 1.75, a reasonable value for this region.

It is worth noting that first locations were not run using the models of Cruz-Atienza *et al*. (2001) and De Barros *et al*. (2008) for the following reasons: (1) the model from Cruz-Atienza *et al*. (2001) includes a low velocity zone, a model property not permitted by Hypocenter, (2) the model from De Barros *et al*. (2008) is similar to the one from Valdés-González and Comité (1994).

Location methods

First locations

A first study locating Popocatépetl earthquakes was reported by Valdés *et al*. (1995). They located 55 earthquakes of the types A, B and AB (VT, low frequency and hybrid events, respectively) using digital seismograms recorded at seven seismic stations. These events, recorded during December 1994 and March 1995, were mainly concentrated below the crater and only three events were located in the southeast region.

In the unpublished work by Valdés-González and Comité (1994), with parts shown in Arámbula-Mendoza *et al*. (2010), nearly 2,000 VT events recorded from 1994 to 2006 below Popocatépetl were located using the Hypocenter program, within a range of about 20 km. They found the events formed two connected clusters, one below the summit (Cluster A) and the other southeast of it (Cluster B) (Fig. 2). Earthquake

sources were distributed at depths between -3 km and 7 km b.s.l. under the crater region, and down to 5 km b.s.l. in the SE-zone. These locations are used in this study for relocation with the genetic search algorithm, called DisLoca, and described in section 5.2. For better comparison, Fig. 3 shows the same 405 events located with Hypocenter, later relocated with DisLoca using the velocity model from De-Barros *et al*. (2008) (Line 1 dark green, dashed, of Fig. 4 (see also section 4)).

Lermo-Samaniego *et al*. (2006) analysed volcano-tectonic earthquakes recorded by a minimum of 5 stations from the Popocatépetl Seismic Network during the period 1994-1999. Their hypocentral locations were calculated using the SEISAN program (Havskov, 2003), with the one-dimensional (1-D) velocity model proposed by Valdés-González and Comité (1994) (see Fig. 4) and a Poisson ratio of Vp/Vs=1.76; coda magnitudes were estimated from parameters, as proposed by Chavacán *et al*. (2004). Lermo-Samaniego *et al*. (2006) verify the existence of the two main clusters mentioned above. Their events have coda magnitudes $M_c < 3.2$ and depths below 12 km, with hypocentral location errors estimated as < 1 km. Based on the asumption that VT-earthquakes under the crater are caused by direct volcanic activity (i.e., magma motion), as proposed by Minakami (1974) and Karpin and Thurber (1987); Lermo-Samaniego *et al*. (2006)

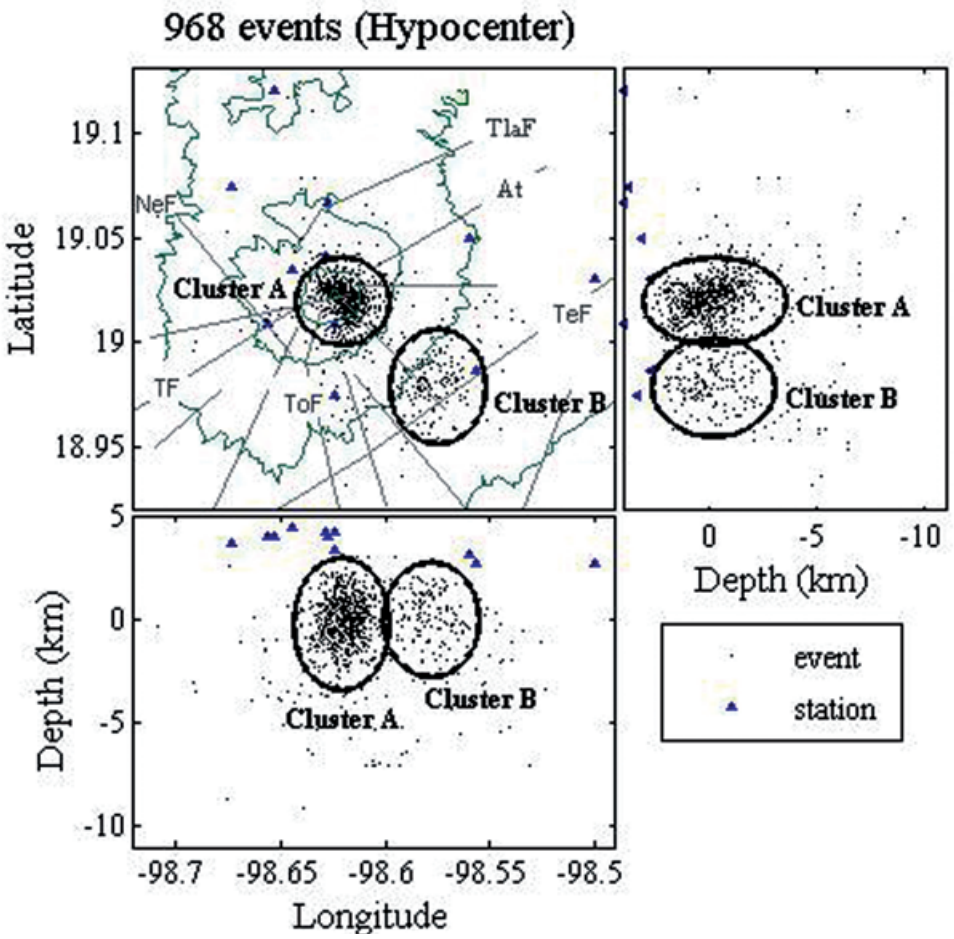

Figure 2. Distribution of 968 VT hypocenters (black points) located with Hypocenter, selected for relocation using DisLoca; see text for event selection criteria. Cluster A and Cluster B are easily identifiable and indicated by black circles. Topography (Isoclines of 2,200, 3,000, 3,800, 4,600 and 5,400 m) is shown by dark green lines (digital models from INEGI), and fault lineations published by Meritano-Arenas *et al*. (1998) are shown as gray lines. We see no correlation between the proposed faults (Meritano-Arenas *et al*., 1998) and the epicentral locations of the VT events. Faults and fissures at Popocatépetl Volcano (Meritano-Arenas *et al*., 1998): Nexpayantla Fissure (NeF) (NW-flank, potential channel for mud and lava flows); Atexca Fault (At) (strike-slip fault sinestral, part of zone of solifluction); Tlamacas Fault (TlaF) (strike-slip dextral, northern limit of the zone of solifluction); Tlaltzompa Fissure (TF) (crossing the central part of the volcanic edice), Espinasa-Perena and Martín-Del-Pozzo (2006) mapped aligned cones toward the NE and SW of the crater; Tetela Fault (TeF) (Southern mountainside, cuts Tochimisolco Fault, covered by recent calcalinic extrusions, cineritic cones to the north); Tochimisolco Fault (ToF) (S-flank,) (Meritano-Arenas *et al*., 1998). Scale: 0.1º Latitude = 11.12 km; 0.1º Longitude = 10.51 km.

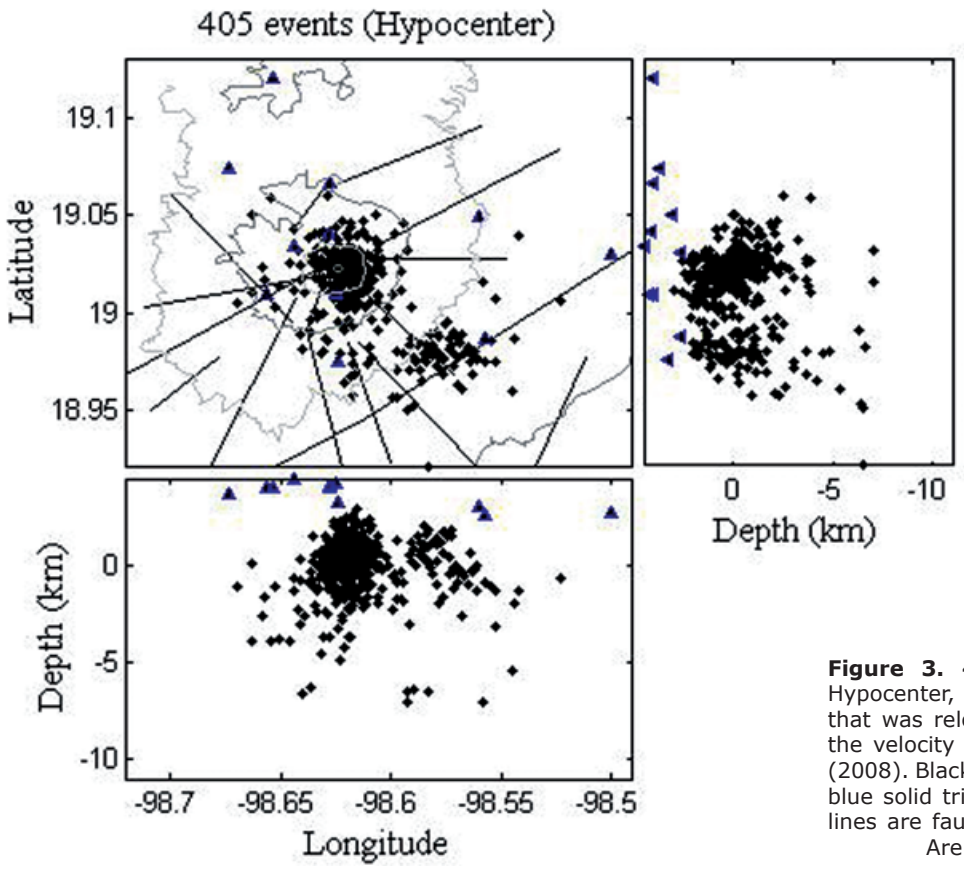

Figure 3. 405 events located with Hypocenter, same selection of events that was relocated with DisLoca using the velocity model of De-Barros *et al*. (2008). Black dots represent VT events, blue solid triangles represent stations, lines are faults proposed by Meritano-Arenas *et al*. (1998).

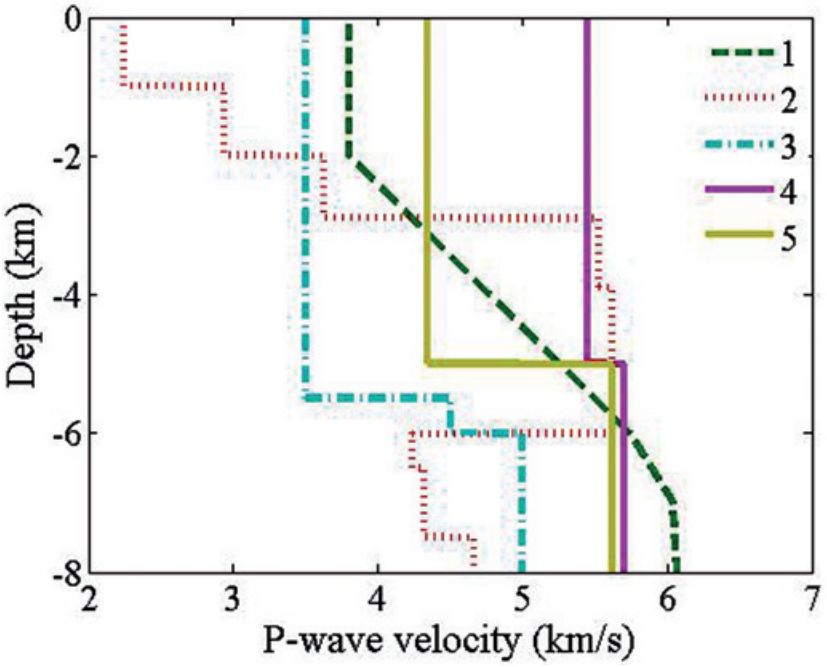

Figure 4. 1-D P-wave velocity models determined for Popocatépetl Volcano: (1) De-Barros *et al*. (2008), (2) Cruz-Atienza *et al*. (2001) and (3) Valdés-González and Comite (1994). For studies on the Mexican Volcanic Belt (MVB), we show the models proposed by (4) Campillo *et al*. (1996) and (5) Valdes *et al*. (1986). See text for description.

proposed that seismicity under the crater could be related to fracture processes in the volcano flanks, as a result of magmatic upwelling.

According to the studies by De la Cruz-Reyna and Siebe (1997); De Cserna *et al*. (1988); Meritano-Arenas *et al*. (1998); Lermo Samaniego *et al*. (2006); Arámbula-Mendoza *et al*. (2010), events in the SE zone are probably tectonic events occurring on a NW-SE striking fault, which according to Arámbula-Mendoza *et al*. (2010) appears to be activated by the movement of rising magma in the Popocatépetl edifice. Lermo-Samaniego *et al*. (2006) associate events in the SE zone to normal faulting in a NW-SE direction that may have been caused by tensional stresses that activated or reactivated a fault system caused by the persistent activity of Popocatépetl during the last 10 years.

The first hypocentral locations obtained by using SEISAN and Hypocenter do not show any relationship to the faults proposed by De Cserna *et al*. (1988) and Meritano-Arenas *et al*. (1998) (except for Tlaltzompa Fissure (TF) (see Fig. 2, where vents are mapped by Espinasa-Perena and Martín-Del-Pozzo 2006) nor do they allow the interpretation of a magma chamber. We will explore the possibility that more sophisticated location algorithms may shed some light on these expected features.

Relocation Method - DisLoca

In order to relocate the events of the Popocatépetl volcano-tectonic catalog data recorded between 1995 and 2006, and preliminarily located with the location program Hypocenter, we applied a recently-developed absolute location algorithm, called DisLoca. DisLoca (Nava, 2010) estimates hypocentral coordinates by finding the hypocenter which results in the minimum L1 (mean absolute) residual between calculated and observed arrival time differences between all recorded P_g and S_g phases, by a genetic search in space, followed by the determination of the origin time. Location determination begins by considering hypocenters at a given grid of strategically-distributed points within and around the station array; it can also include a previously-determined hypocenter for relocation. A given number of children are generated by varying the parent (initial) locations with normally distributed pseudo-random numbers, with X, Y, and Z standard deviations proportional to the corresponding standard deviations for the parent hypocenters and a given mutation probability; other children are constructed as averages of pairs of parents. Next, new parents are chosen from among the entire new population, including parents and children, and the process is repeated until residual and spatial convergence criteria are met for an acceptable location, or until a given number of generations is reached, without meeting the residual creteria, in which case the location is considered unacceptable.

Once an acceptable location is found, the origin time is estimated from the travel times to the stations. The resulting hypocentral parameters are reported, together with arrival time residuals. The average difference time residual is reported as a measure of the fit error, and the space around the preferred hypocenter is explored to determine the X, Y, and Z ranges for which the location error increases by less than a given criterion, which gives a good estimate of the location uncertainty.

DisLoca uses a layered model, and can feature a truncated cone having the first layer's velocity, to roughly model the volcanic edifice. The program accepts station corrections, which allows the possibility of using some selected hypocenter as a master event for the location of other events close to it. The use of arrival time differences, besides reducing the dimension of the search space, makes DisLoca locations more stable in cases of less-than-optimal azimuthal coverage versus straight arrival time fitting. A principal difference between DisLoca and many other common location programs such as Hypo71, Hypocenter or HypoDD, is that DisLoca accounts for station elevation and includes an approximation to the shape and altitude of the volcanic edifice. This is why DisLoca may locate events within the volcanic cone, events that are considered "airquakes" by other programs such as HypoDD or Hypocenter.

Relocation method - HypoDD

In order to compare the results obtained from DisLoca to other relocation results, we applied the double-difference relocation algorithm HypoDD (Waldhauser and Ellsworth, 2000; Waldhauser, 2001). HypoDD is a relative location program based on the double-difference algorithm which uses the double-difference equation:

$$dr_k^{ij} = \left(t_k^i - t_k^j\right)^{\text{obs}} - \left(t_k^i - t_k^j\right)^{cal} \qquad (1)$$

Where dr_k^{ij} is the residual between observed and calculated differential travel times for the two events i and j, recorded at station k. HypoDD minimizes residual double-differences for pairs of earthquakes by adjusting the vector differences between their hypocenters, and determines the interevent distances between correlated events, without need for station corrections (Waldhauser and Ellsworth, 2000; Waldhauser, 2001).

Data

From the recorded digital time series, the P_g and S_g arrival times were measured with a minimum accuracy of 0.05 s and 0.1 s, respectively, due to sharp P and S arrivals from VT earthquakes.

The original locations of VT events compraise around 1,800 events and form two main clusters of about 5 km diameter, one below the summit (Cluster A) and a second SE of the summit zone (Cluster B). Out of this data set we selected 968 events, including 4,321 P-wave phases and 3,009 S-wave phases, for the relocation process (Fig. 2). This selection included events recorded by at least four stations with a minimum weight of 0.1, where 1 is the best and 0 is the worst. The RMS residual error was not chosen as a selection parameter because it results, among other factors, from uncertainties in the 1-D velocity model, which cannot correctly represent all parts of the heterogeneous volcanic body.

Results

Results from DisLoca

The hypocenter relocations obtained by the time-difference genetic search approach, DisLoca, provide a clear new picture of VT events beneath Popocatépetl (compare Fig. 2, Fig. 3 and Figs. 5a, b, c). Out of 968 events, we relocated 331 to 405 volcano-tectonic events, depending on the velocity model applied. Events show at least four P-phases and weights of 0.1 - 1, (see Tab. 1 for details) and were recorded between Nov. 1995 and Dec. 2006. Earthquakes with a final location error higher than 0.1 s were discarded by the location algorithm.

Although DisLoca minimizes the L1 residuals, relocation yielded a substantial reduction in the RMS of the relocated events. The initial weighted RMS values for catalog data were 0.128 s. After relocation, these errors were reduced to 0.045 s (Tab. 1) for the same group of hypocenters.

The number of relocated events differs for the different velocity models used for the inversion (see Figs. 5a, b, c); we relocated 331 events for the velocity model from Cruz-Atienza *et al*. (2001), 386 for the velocity model from Valdés-Gonzáléz and Comité (1994) and 405 events for the velocity model from De-Barros *et al*. (2008). We will base our interpretation on the results using the velocity model from De-Barros *et al*. (2008) (Fig. 5c), as its application resulted in the highest number of relocated events.

Relocated events below the crater area still accumulate in Cluster A, with depths down to 4 km b.s.l. and 7 to 11.4 km b.s.l., with their main occurrence limited to -1.5 to +1 km b.s.l. Relocated events in the southeast zone (about 5 km southeast of the crater), however, are not relocated in a clear Cluster B (see Fig. 1), unlike the originally-located events and as cited by Arámbula-Mendoza *et al*. (2010) and Lermo-Samaniego *et al*. (2006). Events in the southeast zone are relocated in perpendicularly-aligned clusters, with

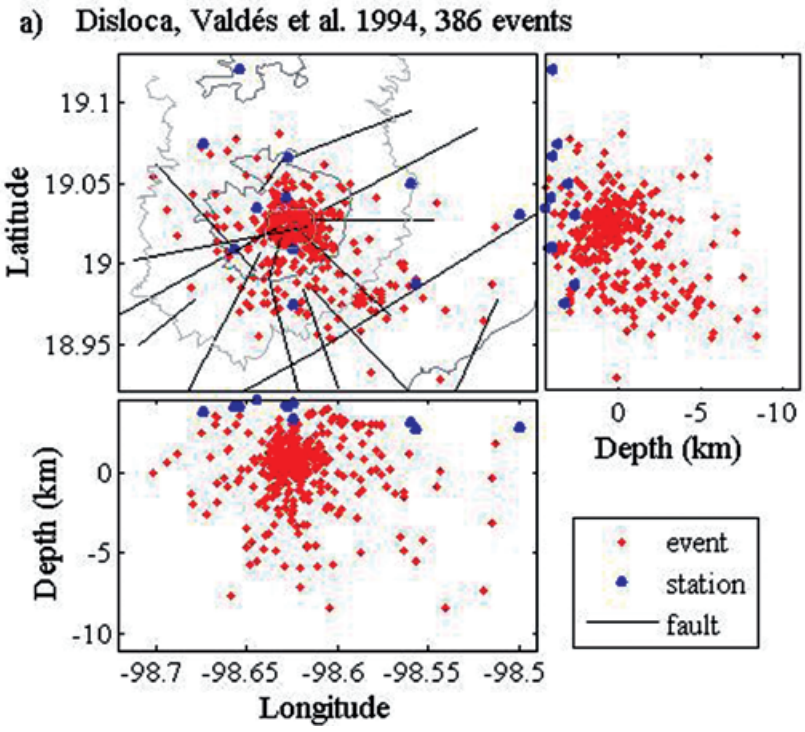

Figure 5. a, b and c: Relocated events down to 11 km depth b.s.l., inverted with the velocity models Valdés-González and Comité (1994) (386 events), Cruz-Atienza *et al*. (2001) (331 events), and De-Barros et al. (2008) (405 events), respectively. Slight differences can be seen in the relocations using different velocity models; see text for discussion. Scale: 0.1 Latitude = 11.12 km; 0.1 Longitude = 10.51 km.

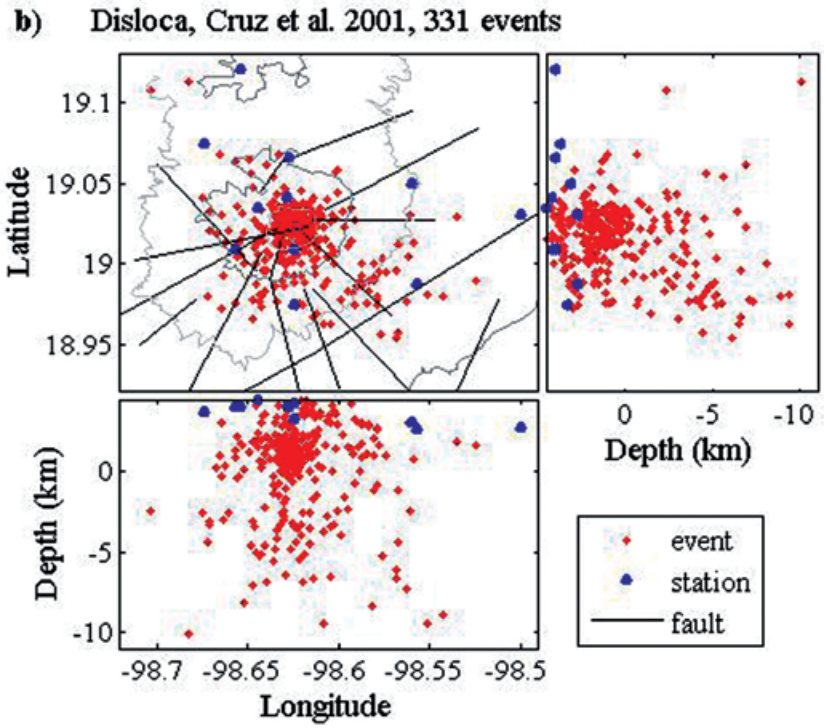

Figure 5b.

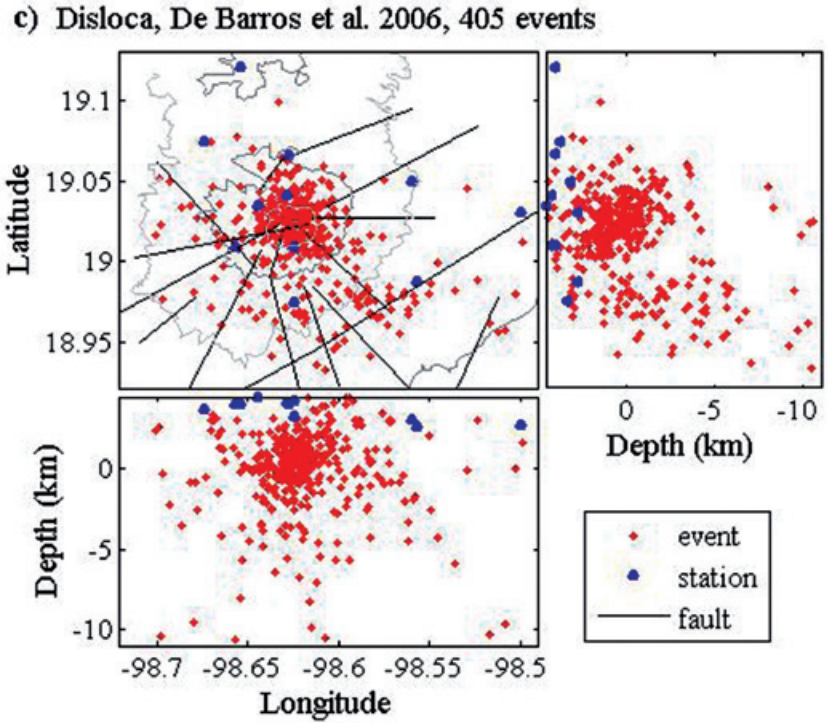

Figure 5c.

NE-SW and NW-SE strikes, marked in Figs. 5c and 253 6a (see § 8). The maximum depth of events in the southeast zone is 4.3 km, with main event occurrence at -1.2 to +0.9 km b.s.l.

We observe a strong correlation in local and temporal event occurrence. It is notable that events recorded in the time period from 1995 to the eruption on 30th June 1997 are relocated mainly in the southern part of Cluster A and to the southeast. A small number of events of this Period 1 are relocated in the northern part of Cluster A, but not in its center (see Figure 6a). We observe as well a strong correlation between event occurrence and volcanic episodes, which are defined after Arámbula-Mendoza (2007). Table 2 shows the 13 volcanic episodes differentiated in time and their mode of

Table 1. The adjusting error of the time differences between stations (dTerr) in seconds and root mean square travel time residual (TTRMS) in seconds for the relocated events for all three velocity models from Valdés-González and Comité (1994); Cruz-Atienza *et a*l. (2001); De-Barros *et al*. (2008).

Velocity Model	dTerr	TTRMS	Relocated events	Input events
Valdés-González and Comité (1994)	Mean: 0.0548 Min: 0 Max: 0.100	Mean: 0.0460 Min: 0 Max: 0.104	386	968
Cruz-Atienza *et al*. (2001)	Mean: 0.053 Min: 0 Max: 0.099	Mean: 0.0446 Min: 0 Max: 0.104	331	968
De-Barros *et al*. (2008)	Mean: 0.0548 Min: 0 Max: 0.099	Mean: 0.0457 Min: 0 Max: 0.1048	405	968

Table 2. 13 volcanic episodes from 1995 to 2006. Description changed after Árambula-Mendoza (2007).

Volcanic episodes	Time (Month/ Year)	Description	Location of events > 3 km from crater (azimuthal degree)	Depth general b.s.l.(km)	Depth crater zone a.s.l.(km)	Depth SE zone a.s.l.(km)
1	02/04/95-03/03/96	Fumarolic phase and ash	30, 100, 330	+2.4 to -1.5		
2	04/03/96-30/09/96	Dome construction	135-230	+4.5 to -1.9	+2.9 to -1.9	
3	01/10/96-18/08/97	Ash and Explosions 260, 360	Most: 120, Or: 90,	+4 to -12	+4 to -1.6	+3 to -0.8
4	19/08/97-24/12/97	Dome construction, effusive	140, 170, 270, 350-360	+4 to -9.2	+4 to -2 to	+3.0 -0
5	25/12/97-22/11/98	Explosions, Energy accumulation	135-180 and 270-40	+3.2 to -9.7	+3.2 to -2.6	+3.0 to -2.3
6	23/11/98-03/01/99	Very explosive	45, 180, 220, 320	+4.5 to -6.8	+4.5 to -0.6	
7	04/01/99-03/09/99	Post eruptive and relaxation	130, 170-220, 280-40	+4.2 to -7.1	+4.2 to -2.2	+1 to -4.5
8	04/09/99-15/09/00	Relaxation (period of repose)	135-160, 200-270	+4.5 to -11.4	+4.5 to -2.6	+3 to -1.9
9	16/09/00-10/12/00	Recharge	190	+4.4 to -5.6	+4.4 to -5.6	
10	11/12/00-23/01/01	Dome growth and eruptions	200, 310	+4.5 to -4.5	+4.5 to -0.8	
11	24/01/01-31/05/02	Post eruptive and small dome growths	120-160, 220, 190, 260-280	+4.5 to -4.6	+4.5 to -3.6	+3 to -3.3
12	01/06/02-31/12/03	Explosions and Relaxation	130-270	4.4 to -9.9	4.4 to -9.9	+1.2 to -4.3
13	01/01/04-31/12/06	Relaxation	190, 270, 360	+4.5 to -10.5	+4.5 to -3.5	-2

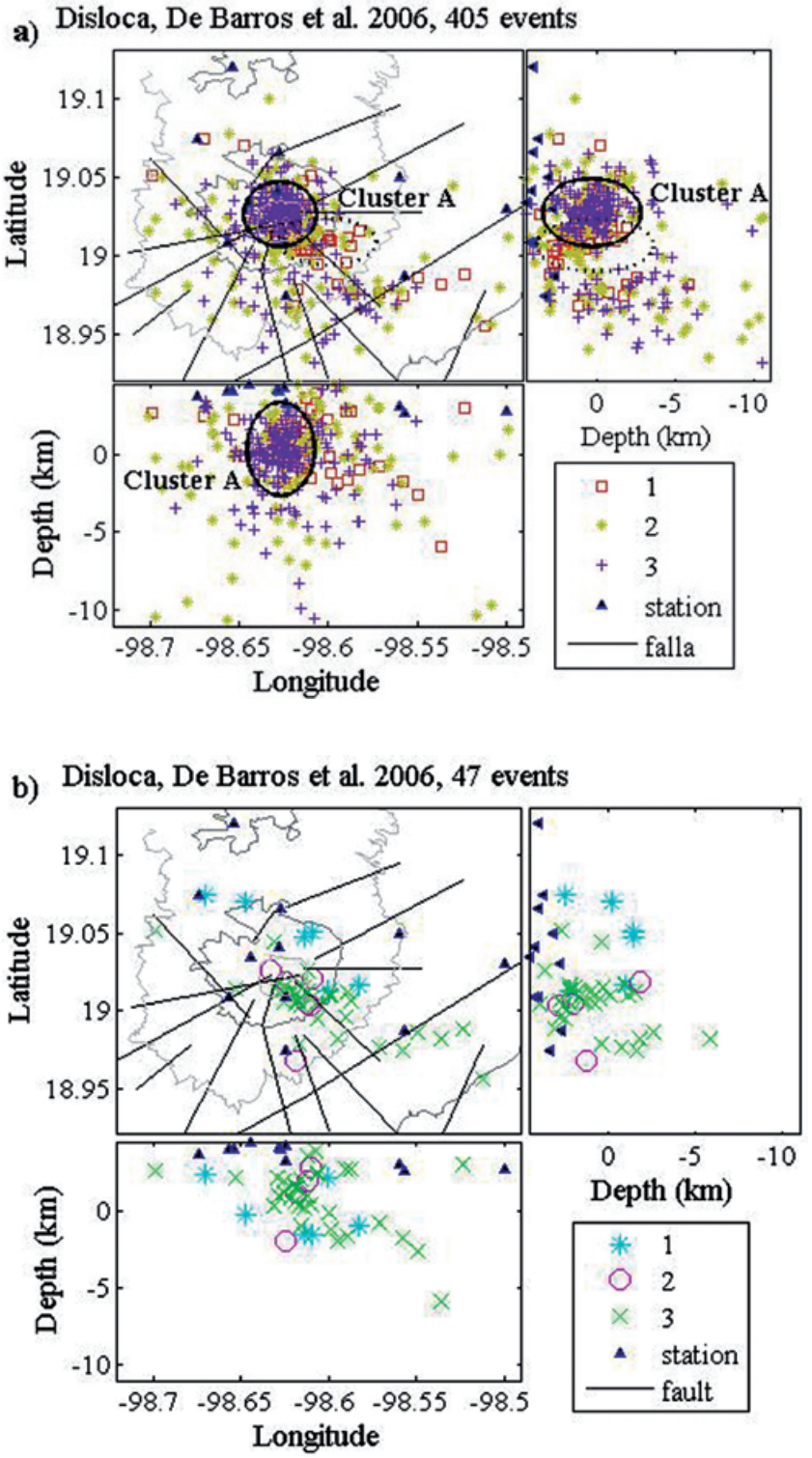

Figure 6. Occurrence of relocated VT events with the model from De-Barros *et al*. (2008): a) Three volcanic periods (see numbers 1-3 in legend) separated by the two main explosive eruptions on 30th of July 1997 (VEI = 2-3) and 22th of January 2001 (VEI = 3-4). We outline Cluster A (dark circle), as well as the zone of accumulation of events of volcanic Period 1 (dashed circle). Cluster B (southeast of the crater) cannot be identified in the relocations. b-f): 13 different volcanic episodes (see numbers 1-13 and different symbols in legend). We observe a strong correlation of episodes with event location. See text and Table 2 for descriptions. For better differentiation of the 13 episodes, they are plotted in three different graphics: b) Episodes 1-3, c) Episodes 4-6 and d) Episodes 7-9, e) Episodes 10-11, f) Episodes 12-13.

activity. In Figure 6b-f we observe that Cluster A (shown in Figure 6a) consists of relocated events from nearly all thirteen episodes, except from Episode 1. Episode 1 is characterized by gas and ash emission and its events are relocated in a NW-SE aligned cluster of about 10 km length located north and east from the central part of the volcano. Episode 3 is a phase of moderate ash emission, as well as spasmodic tremors. The events of Episode 3 are grouped into two clusters, one located 1.5 km south of the crater and a second aligned in an E-W direction begining at 4 km south of the crater and up to 9 km southeast of it.

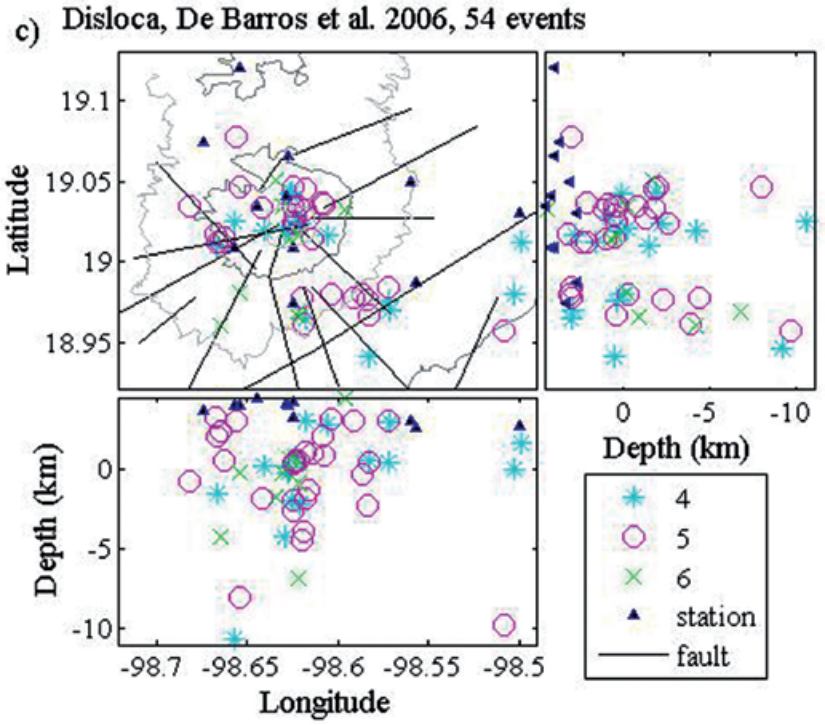

Figure 6c.

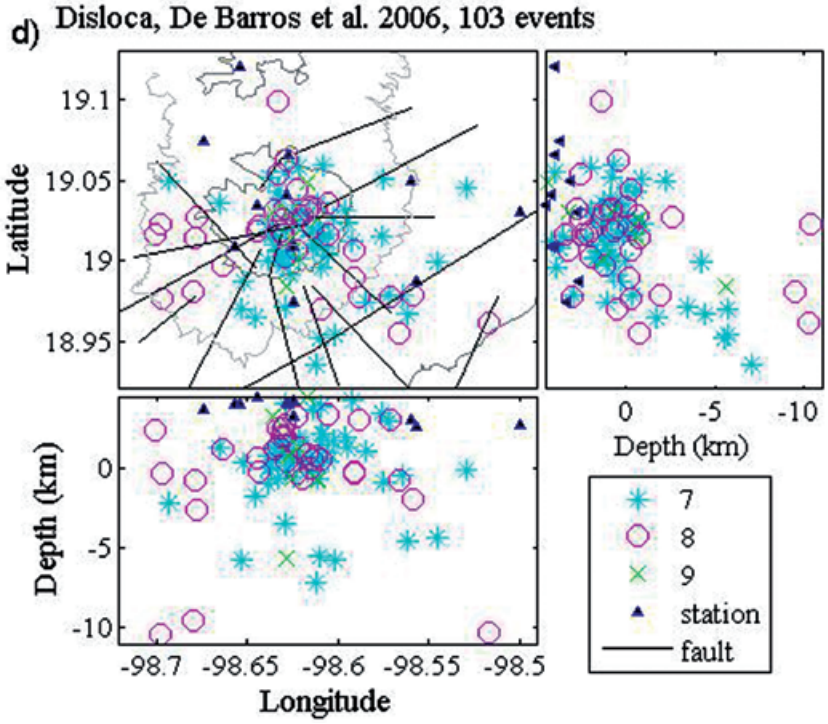

Figure 6d.

Events to the southeast consist mainly of events from Episodes 5 and 12, which are characterized by a high quantity of volcanic explosions and a subsequent relaxation phase (return to a period of repose/rest). One or two events located in the southeast are from Episodes 7 (post-eruptive and relaxation phase), 8 (relaxation phase) and 11 (post-eruptive phase (refers to the large explosive event 22 Jan. 2001 and small domes).

Events from Episodes 7 and 12, post-eruptive and relaxation phases, are located 4 to 8 km south of the crater region. They are located at

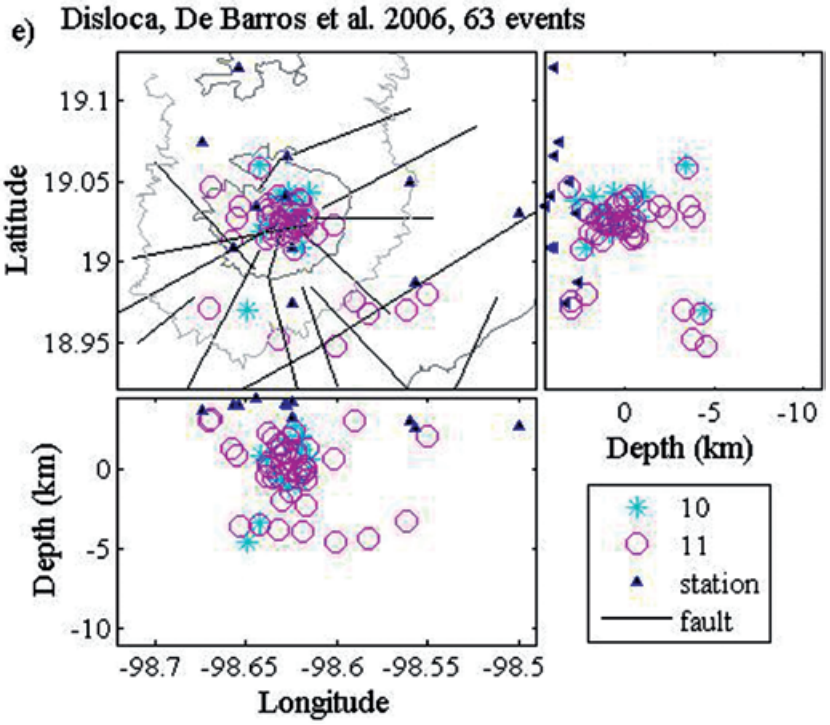

Figure 6e.

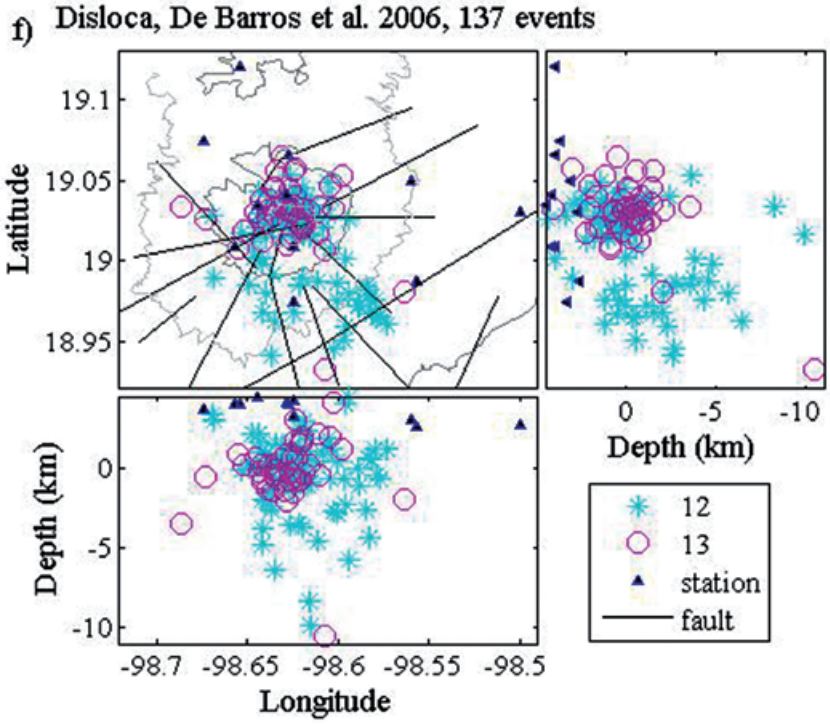

Figure 6f.

depths from -3.5 to 10.5 km b.s.l., and therefore more than 6 km deeper than events located on the NW-SE and NE-SW striking faults in the SE region. Events located south of the central volcanic region are from episodes of dome construction and eruptions: (4), 5, 6, (9), 10, 11, (13), where episodes marked in parentheses contain only one event, others two or three events.

Figure 7 shows the events from Episodes 3, 10 and 12 in 3-D cross-section, in order to display inclined event alignments not visible from the map views shown in Fig. 6. The events are inclined, suggesting normal or inverse faults (Figs. 6 and 7).

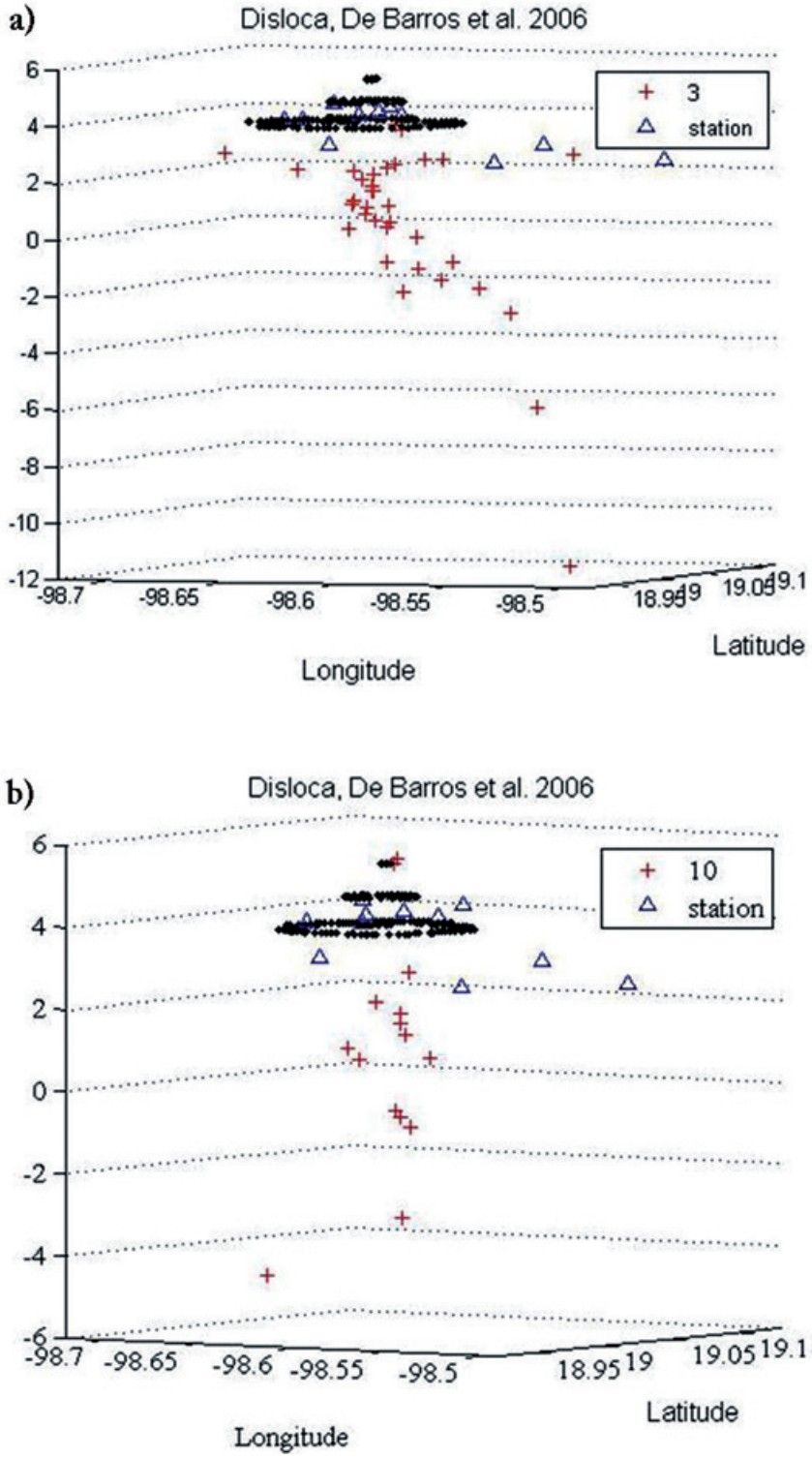

Figure 7. Views from the SE and SW, show 3-D hypocenter alignments; we show examples of Episodes 3, 10 and 12. a) Events of Episode 3, view from SE. b) Events of Episode 10, view from SE. c) Events of Episode 12, view from SW. Scale: 0.1 Latitude = 11.12 km; 0.1 Longitude = 10.51 km. Topography in black circles: 5,400 m, 4,600 m, 3,800 m.

Differing station corrections for different ray paths can indicate the presence of low or high velocity regions, such as magmatic chambers or conduits. DisLoca permits the estimation of station corrections from the mean (re)location error (in seconds) and its standard deviation for P- and S-wave rays. Here, we show station correction examples for events located with the velocity model from De-Barros *et al*. (2008). We estimated the station correction for each station for the entire dataset (Table 3) and then searched for differences in station corrections as functions of the earthquake's occurrence in time and location (Tables 1, 3 and 4). We observe a high variation in values of station corrections in space and time, which does not allow for a systematic location including station correction.

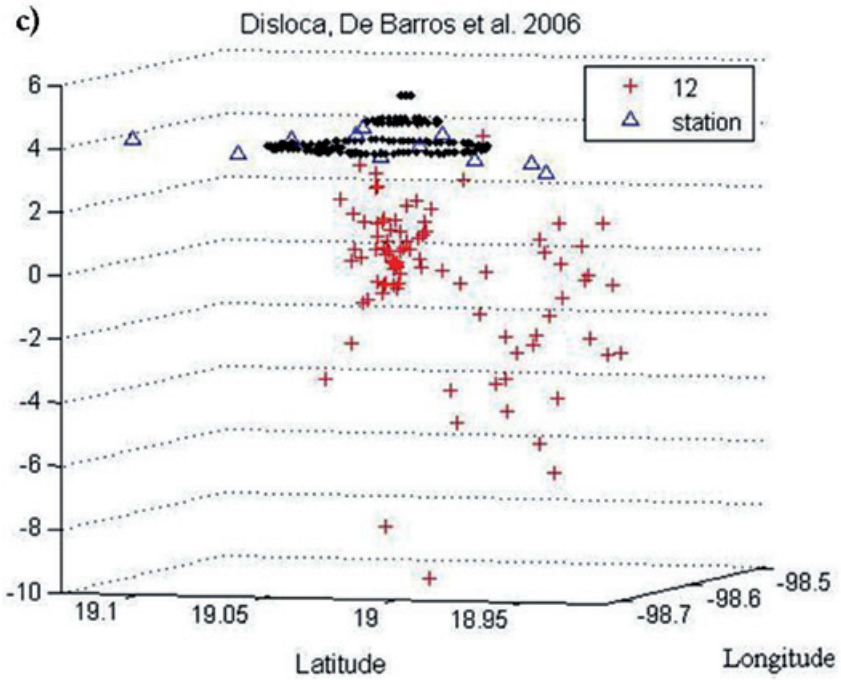

Figure 7c.

Table 3. Comparison of different station corrections in seconds for a) rays passing and b) not passing below the crater region. Station corrections are determined for the entire recording time (1995-2006) and for three volcanic periods, divided by two main eruptions on 30th June 1997 and 22nd January 2001. The last column shows the differences in station correction for different ray paths at different stations. Station corrections for rays passing through the region below the crater are not similar, neither for the S- and P-phases, nor for the volcanic periods. See text for description.

Station correction (in seconds) for rays passing and not passing below the crater region								
	a) Rays below Crater			**b) Rays not below Crater**				
	Station Corr. 1995-2006			Station Corr. 1995-2006			**Difference**	
PPQ-P	0.0002			0.0133			0.0131	
PPQ-S	-0.0085			-0.0104			0.0019	
PPT-P	0.0000			-0.0116			0.0115	
PPT-S	0.0200			0.0194			0.0006	
	1995-1997	1997-2001	2001-2006	1995-1997	1997-2001	2001-2006	1997-2001	2001-2006
PPQ-P	/	-0.0139	-0.0099	0.0501	-0.0073	-0.0143	0.0065	0.0044
PPQ-S	/	0.0085	-0.0012	/	-0.0058	-0.0005	0.0133	0.0007
PPT-P	/	0.0008	-0.0244	-0.0120	-0.0112	-0.0231	0.0103	0.0013
PPT-S	/	0.0210	0.0475	0.0066	0.0130	0.0423	0.0080	0.0052

Table 4. Station corrections (in seconds) for three different volcanic periods: 01. Jan. 1995 - 30. Jun. 1997 (Stat. Corr. 1), 1. Jul. 1997 - 22. Jan. 2001 (Stat. Corr. 2), 23. Jan. 2001 - 31. Dec. 2006 (Stat. Corr. 3), and the differences between them. Station correction was estimated from the Mean error ε (s) and the standard deviation. A change in station correction occurs with time.

Station & Phase	Stat. Corr. 1995-1997 (1)	Station & Phase	Stat. Corr. 1997-2001 (2)	Station & Phase	Stat. Corr. 2001-2006 (3)	Difference (1) and (2)	Difference (2) and (3)
PPA P	0.0155	PPA P	0.0289			0.0134	
		PPA S	-0.0198				
PPN P	0.0082	PPN P	0.0199			0.0117	
		PPJ P	0.0088	PPJ P	-0.0283		0.0371
		PPJ S	0.0011	PPJ S	-0.0081		0.0092
PPX1 P	-0.0060	PPX1 P	-0.0014			0.0046	
PPX1 S	-0.0041	PPX1 S	-0.0347			0.0306	
		PPX2 P	-0.0101	PPX2 P	0.0011		0.0112
		PPX2 S	-0.0057	PPX2 S	0.0135		0.0192
		PPP1 P	-0.0140				
PPP1 P	0.0072	PPP1 S	0.0207			0.0135	
PPP1 S	0.0233	PPP2 P	-0.0002	PPP2 P	0.0065	0.0235	0.0067
		PPP2 S	-0.0070	PPP2 S	-0.0043		0.0027
PPQ P	0.0020	PPQ P	0.0153	PPQ P	-0.0004	0.0133	0.0157
PPQ S	-0.0022	PPQ S	-0.0156	PPQ S	0.0169	0.0134	0.0325
PPM P	-0.0101	PPM P	-0.0290	PPM P	0.0156	0.0189	0.0446
PPM S	0.0193	PPM S	0.0132	PPM S	0.0137	0.0061	0.0005
PPT P	-0.0089	PPT P	-0.0123	PPT P	0.0183	0.0034	0.0306
PPT S	0.0269	PPT S	0.0086	PPT S	-0.0289	0.0183	0.0375
PPC P	0.0040	PPC P	-0.0013	PPC P	-0.0039	0.0053	0.0026
PPC S	-0.0419	PPC S	-0.0063	PPC S	0.0068	0.0356	0.0131
		PPS P	0.0013				
PPB P	-0.0113						
PPB S	0.0421						

Results from HypoDD

With HypoDD, depending on the velocity model applied, we relocated between 430 and 561 out of 739 events, which were preselected by a program that searches for possible pairs of earthquakes (Fig. 8a). Events were automatically discarded by the relocation algorithm if they were badly connected or if their depths decreased to less than the subsurface (airquakes, 3 km above sea level in the case of Popocatépetl).

There is a strong dependence on the velocity model for HypoDD, which is clearly observed when comparing the results obtained by applying the velocity model of Cruz-Atienza *et al*. (2001), which includes a low velocity zone, with the results obtained by applying the velocity models of Valdés-González and Comité (1994) and De-Barros *et al*. (2008) (Fig. 8).

In the map views of the relocation results, relocation concentrates the events in two clusters (Cluster A and B) for all three velocity models (map views, Fig. 8). We observe no visible alignment in event distribution correlating to the fault zones, as indicated by De Cserna *et al*. (1988) and Meritano-Arenas *et al*. (1998). The area of event distribution was slightly reduced, compared to the initially located events in Figure 2. Events are located at depths of +3 and -5 km b.s.l. The value of the maximum depth was diminished by only 1 km (5 km b.s.l. located to 4 km b.s.l. relocated).

The velocity model of Cruz-Atienza *et al*. (2001) shows a horizontal event accumulation at -1.5 to 0 km depth b.s.l. including events from below and around the crater region and the southeastern region. Below 312 the crater we image an inclined "conduct" of events at depths of -2 to 4.5 km b.s.l. and a horizontal diameter of about 2 km.

The relocated Cluster A, using HypoDD and the models of Valdés-González and Comité (1994) and De-Barros *et al*. (2008) looks pretty similar to the Cluster A resulting from the relocation using DisLoca.

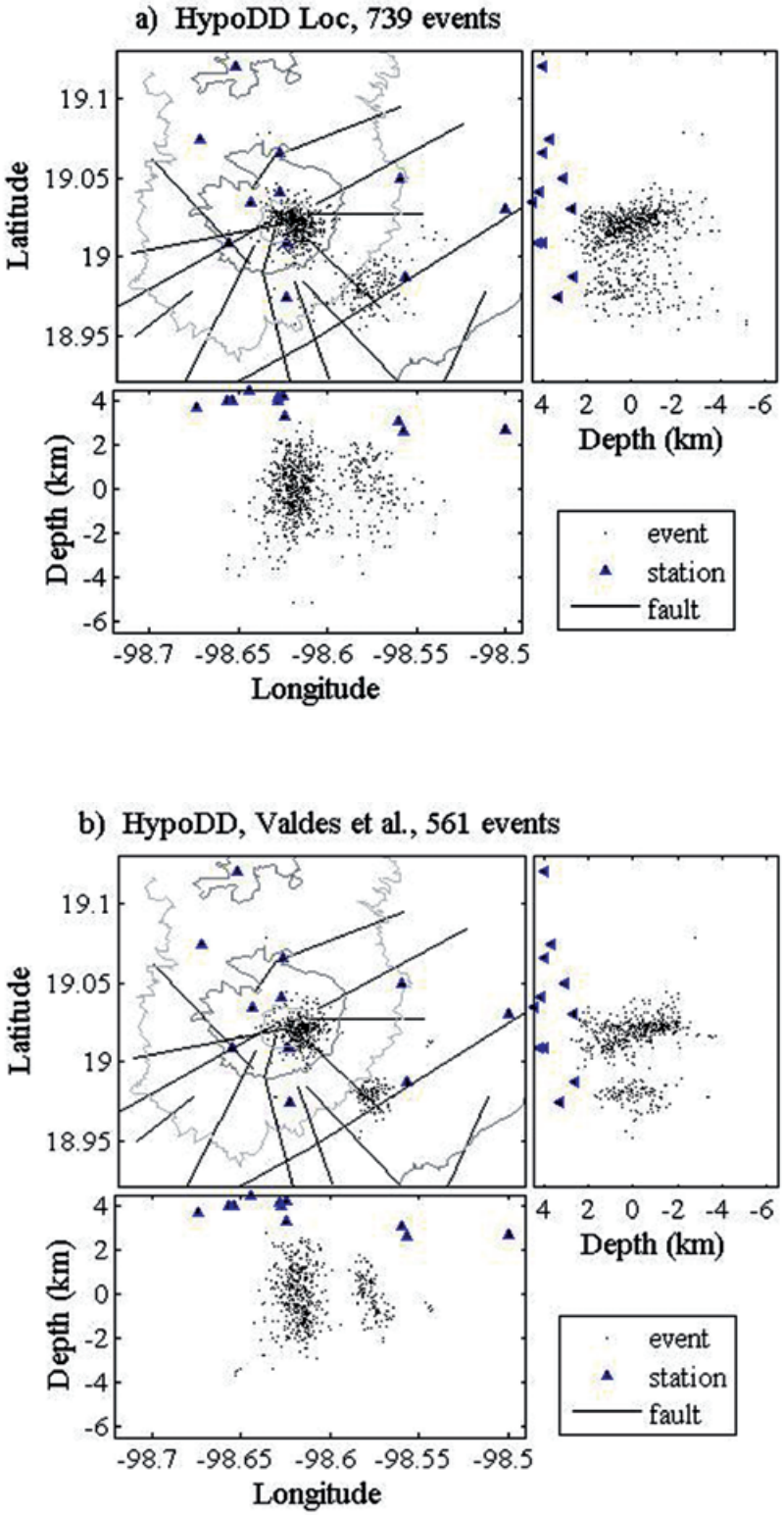

Figure 8. Events before and after relocation with the DD algorithm HypoDD: a) Distribution of 739 events before being relocated with HypoDD. Events were selected using the entire data set and a preprogram offered in the DD algorithm which selects pairs of events. b), c) and d): Relocated events, inverted with the velocity models Valdés-González and Comité (1994), Cruz-Atienza *et al*. (2001) and De-Barros *et al*. (2008), respectively. Large differences can be seen in the relocations, comparing b) and c) to d). See text for discussion. Scale: 0.1º Latitude = 11.12 km; 0.1º Longitude = 10.51 km.

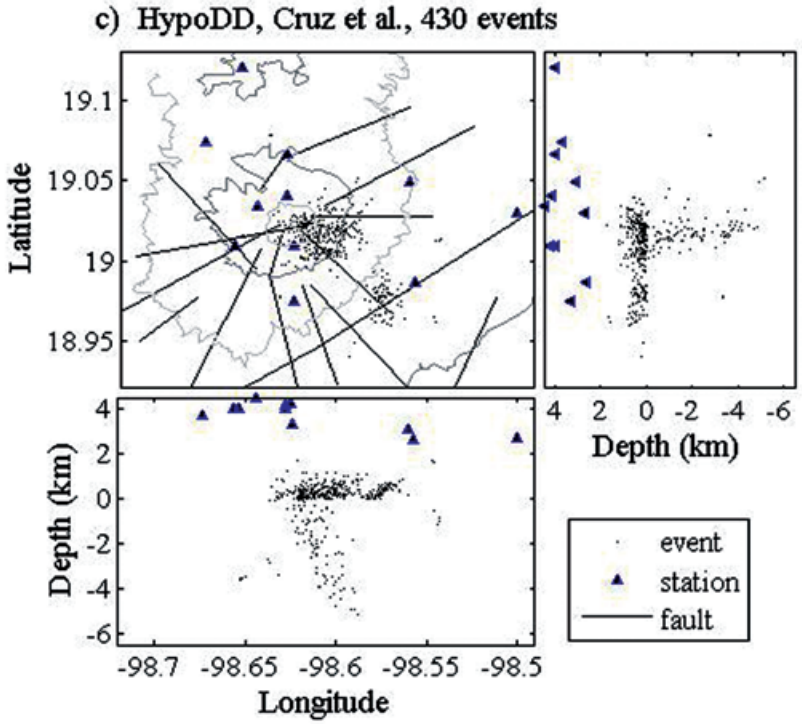

Figure 8c.

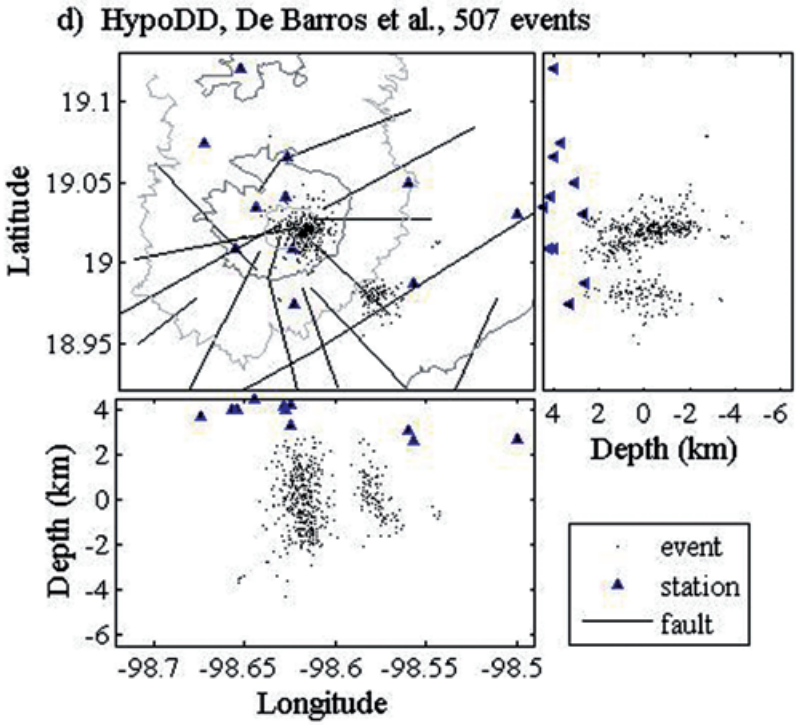

Figure 8d.

Discussion and Conclusions

This study applied a genetic algorithm location method to relocate 331, 386 and 405 volcano-tectonic events, depending on the velocity model applied, recorded between Nov. 1995 and Dec. 2006 beneath Popocatépetl Volcano, and initially located using the program Hypocenter. These results are supplemented by applying the double-difference algorithm HypoDD (Waldhauser and Ellsworth, 2000) on the initially event locations.

Different relocation results between HypoDD and DisLoca may arise from differences in the algorithms: (1) DisLoca includes topography and station elevation and may accept events that are discarded as airquakes in HypoDD, (2) the genetic algorithm searches for the global optimum while the least squares regression applied in the double-difference algorithm may fall easily in a local optimum. While the RMS in the relocation with DisLoca gets diminished by nearly one third, the RMS in the HypoDD relocation increased from 0.18 s to ~ 0.3 s. The most probable reason for this increase is the lack of waveforms, which may enhance relocation results significantly, as clearly emphasized by Waldhauser and Ellsworth (2000) and Waldhauser (2001).

Comparing the relocation results obtained by DisLoca (Figs. 5 and 6) with those obtained using HypoDD (Fig. 8) clearly shows that the events relocated using the genetic algorithm are aligned and may image predicted fault zones. Aligned epicenters are important because they may indicate strain localization within the volcanic edice, which in turn may indicate increased local risk of collapse. Having the alignments coincide with known faults makes them doubly important. Relocated events using HypoDD, however, result in two main spherical or plate-shaped clusters without any event-alignments. Nearly-spherical shapes were derived using similar velocity models of Valdés-González and Comité (1994) and De-Barros *et al*. (2008), while plate-shaped clusters were derived using the velocity model of Cruz-Atienza *et al*. (2001), which includes a low velocity zone from 3 to 6 km b.s.l. The high dependence on the velocity model using HypoDD is another indication of the instability of the relocation results using the double-difference algorithm with our available data. Hence, we will discuss the results obtained by the genetic algorithm location method DisLoca in more detail.

The number of acceptable relocated events using DisLoca differs depending on the velocity model used during the inversion (see Fig. 4 and Figs. 5a, b, c: 331 events using the Cruz-Atienza *et al*. (2001) model, 386 events using the Valdés-González and Comité (1994) model and 405 events using the De-Barros *et al*. (2008) model). The RMS error was considerably improved from 0.128 s to 0.045 s. These relocations provide a picture of the spatial and temporal patterns of this seismicity.

Events from the first locations with Hypocenter were relocated slightly differently in the relocation process using DisLoca. This is clearly visible in the two main clusters determined using the first locations, Cluster A below the crater and Cluster B in the southeast. Cluster A is still distinguishable in the relocation, but the former clear accumulation of Cluster B is relocated in two aligned linear clusters extending SE-NW, NE-SW, revealing probable faults in direction of the axes of the regional stress field, as previously determined by Meritano-Arenas *et al*. (1998) and De-Cserna *et al*. (1988).

We also observe a clear correlation between event location and volcanic episodes (Tab. 2 and Figs. 6a-f). Events produced during dome construction or eruptive phases occur at different depths than events caused during relaxation. Typical depths for events produced during dome construction are: -4.5 to +2 km b.s.l., while events during explosion phases are relocated to deeper areas, at -3 to +10 km b.s.l.

The relocated aligned clusters, which we interpret as faults, coincide with a special type of volcanic activity, limited in time. In Figures 7a-c, we show the Episodes 3, 10 and 13 inclined aligned structures, which we interpret as faults. These alignments are only seen from the SE or SW direction, in accordance with the regional stress field.

Faults were confirmed from the studies of Meritano-Arenas *et al*. (1998) and De-Cserna *et al*. (1988) are (Figure 6): Tetela Fault and SE-NW fault are both imaged by alignments of events from volcanic Episode 11 (post eruptive and construction of small domes) and Episode 12 (small explosions and relaxation). Tlamacas Fault can be confirmed by aligned clusters from Episodes 7 (post eruptive and relaxation) and 8 (relaxation). Events of Episode 8 image Tlaltzompa Fissure and a W-E striking fault proposed by De-Cserna *et al*. (1988); Espinasa-Perena and Martín-Del-Pozzo (2006) mapped vents SW and NE of the crater, where Tlaltzampa Fissure and Atexca Fault are proposed by Meritano-Arenas *et al*. (1998) and De-Cserna *et al*. (1988); this is why Atexca Fault is better dened as a ssure than a fault. Relocated events from Episodes 2 (dome construction), 3 (ash and explosions), 4 (dome construction, effusive) and 5 (explosions and energy accumulation) are found to form aligned clusters about 5-10 km south of the crater; these assumed faults strike E-W and N-S.

We observe a large number of aligned event clusters that are not included in the areal-pictures-study from Meritano-Arenas *et al*. (1998) (Fig. 6). These formations may be interpreted as hidden faults, but we restrict our interpretation to those shown in Figure 7, to avoid over interpretation.

Zones where seismicity is lacking are of importance, as they may indicate areas of

hot or molten material, such as small magma reservoirs. At depths shallower than 4 km b.s.l., we observe a strong decrease in seismic events; in agreement with studies from e.g., Espíndola *et al*. (2003); Atlas *et al*. (2006) and Roberge *et al*. (2007), a larger magma body or presence of magma could be interpreted below that area. We observe as well areas of no seismicity, e.g., below the crater at -2 km b.s.l., that may be explained by the fact that several significant changes occur at shallow depths (1-3 km) in the highly fractured upper part of Popocatépetl (Novelo Casanova *et al*., 2007).

Observations on the agreement of event location and volcanic behavior indicate that the behavior of magmatic material is predictable, after observing several known patterns. Faults often become activated by magma movement, as proposed for the southeast fault zone by Lermo-Samaniego *et al*. (2006) and Arámbula-Mendoza *et al*. (2010). But faults may be activated as well in times of volcanic relaxation, as is the case for Episode 8, for fault zones west of the volcano (Fig. 6c). Although we observe some correlation between the location of the VT seismic events and previously proposed faults, we do not find large concentrations of earthquakes associated with the SE faults, which could indicate a weakening or future collapse of the volcano edifice, and that thus would represent a volcanic risk in the near future. Based on the thesis of Ramirez-Olvera (2003) and the work of Novelo-Casanova *et al*. (2007), we conclude that a shallow (< 3 km) earthquake of magnitude 4.5 to 5 is necessary, to create a risk of collapse or to create a fissure. The earthquake that produced the flank collapse at Mount Saint Helens, for example, had a magnitude of 5.1 (e.g., Mullineaux and Crandell, 1981). The possibility of an earthquake of magnitude 4.5 to 5, while unlikely, cannot be excluded. In the past, the volcano has collapsed to the south and south-east (e.g., Siebe and Macías, 1997). It is possible that this is the mechanism that may occur in the future.

Acknowledgements

We want to thank the volcano monitoring group of CENAPRED (Nacional Center for Disaster Prevention of Mexico), for keeping the seismic monitoring network at Popocatépetl Volcano. Part of this project was funded by the CONACYT (National Council of Science and Technology of Mexico). Thanks also go to Christine Gans and two anonymous reviewers who provided helpful criticisms of the manuscript.

Bibliography

Arámbula-Mendoza R., 2007, Estado de esfuerzos en el volcán Popocatépetl obtenidos con mecanismos focales en el periodo de actividad de 1996 a 2003 . Tesis de maestría Instituto de Geofísica, UNAM Mexico.

Arámbula-Mendoza R., Valdés-González C., Martínez-Bringas A., 2010, Temporal and spatial variation of the stress state of Popocatépetl volcano, Mexico. *J. Volcan. Geoth. Res.*, 196 , 156-168.

Arciniega-Ceballos M.A., González C.V., Dawson P., 2000, Temporal and spectral characteristics of seismicity observed at Popocatépetl volcano, central Mexico. *J. Volcan. Geoth. Res.*, 102 , 207-216.

Atlas Z.D., Dixon J.E., Sen G., Finnya M., Martín del Pozzo A.L., 2006, Melt inclusions from Volcan Popocatepetl and Volcan de Colima, Mexico: Melt evolution due to vapor-saturated crystallization during ascent. *J. Volcan. Geoth. Res.*, 153 , 221-240. Doi:10.1016/j.jvolgeores.2005.06.010.

Campillo M., Singh S., Shapiro N., Pacheco J., and Herrmann R., 1996, Crustal structure South of the Mexican Volcanic belt, based on group velocity dispersion. *Geofísica Internacional*, 35 , 361-370.

Chavacán M., Lermo J., Quintanar L., 2004, Determinación de una escala de magnitud para temblores corticales en la parte central del Cinturón Volcánico Mexicano. In: *I Conf. Int. Peligrosidad e Ingeniería Sísmica.* Santiago de Cuba, Cuba: Universidad de Oriente. CD.ROM.

Chouet B.A., 1996, Long-period volcano seismicity: Its source and use in eruption forecasting. *Nature*, 380 , 309-316.

Cruz-Atienza V., Pacheco J., Singh S., Shapiro N., Valdés C., Iglesias A., 2001, Size of Popocatépetl volcano explosions (1997-2001) from waveform inversion. *Geophy. Res. Lett.*, 28, 4,027-4,030.

De la Cruz-Reyna S., Siebe C., 1997, Volcanology: The giant Popocatépetl stirs. *Nature*, 388, 227.

De la Cruz-Reyna S., Yokoyama I., Bringas A.M., Ramos E., 2008, Precursory seismicity of the 1994 eruption of Popocatépetl Volcano, Central Mexico. *Bull. Volc.*, 70, 753-767. Doi:10.1007/s00445-008-0195-0.

De-Barros L., Pederson H., Métaxian J., Valdés-González C., Lesage, P. (2008). Crustal structure below Popocatépetl Volcano (Mexico) from analysis of Rayleigh waves. *J. Volcan. Geoth. Res.*, 170 , 5-11.

De-Cserna Z., Fuente-Duch M., Palacios-Nieto M., Trial L., Miltre-Salazar L.M., Mota-Palomino R., 1988, Estructura geológica, gravimétrica, sismicidad y relaciones geotectónicas regionales de la cuenca de México. Instituto de Geología, UNAM. Bolletin 104.

Ego F., Ansan V., 2002, Why is the Central Trans-Mexican Volcanic Belt (102-99ºW) in transtensive deformation?, *Tectonophysics*, 359, 189-208.

Espinasa-Perena R., Martín Del Pozzo A.L., 2006, Morphostratigraphic evolution of Popocatépetl volcano, Mexico. *GSA Special Papers*, 402, 115-137. Doi:10.1130/2006.2402(05).

Espíndola J.M., Godínez M.D.L., Espíndola V.H., 2004, Models of ground deformation and eruption magnitude from a deep source at Popocatépetl Volcano, Central Mexico. *Nat. Haz.*, 31, 191-207.

Espíndola J.M., Macías J.L., Godínez M.L., 2003, Un modelo físico de cámara magmática para la estimacion de los cambios premonitorios en sísmicidad y deformación esperados en volcanes activos. *Geos*, 14 , 356.

Fries C.Jr., 1965, Geología de la Hoja Cuernavaca, Estados de Morelos, México, Guerrero y Puebla. Instituto de Geofísica, Universidad Nacional Autónoma de México. Carta Geológica de México, scale 1:100 000.

Geiger L., 1910, Herdbestimmung bei Erdbeben aus den Ankunftszeiten. *Koenigliche Gesellschaft der Wissenschaften zu Goettingen*, 4, 331-349.

Got J.-L., Fréchet J., 1994, Deep fault plane geometry inferred from multiplet relative relocation beneath the southflank of Kilauea. *J. Geophys. Res.*, 99 , 15,375-15,386.

Havskov O.L.J., 2003, SEISAN: The earthquake analysis software, version 8.0 . Department of Earth Science, University of Bergen (ed.), 250 p. Bergen, Norway.

Ito A., 1985, High resolution relative hypocenters of similar earthquakes by cross-spectral analysis method. *J. Phys. Earth*, 33 , 279-294.

Jordan T.H., Sverdrup K.A., 1981, Teleseismic location techniques and their application to earthquake clusters in the south-central Pacic. *Bull. Seis. Soc. Am.*, 71, 1,105-1,130.

Karpin T., Thurber C., 1987, The relationship between earthquake swarms and magma transport: Kilauea Volcano, Hawaii. *P. App. Geophys*., 125 , 971-991.

Klein F.W., 1985, User's Guide to HYPOINVERSE, a Program for VAX and Professional 350 Computers to Solve for Earthquake Locations. Open-File Report 85-515 U.S. Geological Survey.

Lee W., Lahr J., 1972, HYPO71: A computer program for determining hypocenter, magnitude, and first motion pattern of local earthquakes. U.S. Geological Survey. Open File Report.

Lermo Samaniego J., Antayhua Vera Y., Chaván Avila M., 2006, Análisis de la actividad en el volcan Popocatépetl (México) durante el periodo 1994-1997. *Bol. Soc. Geol. México*, pp. 253-257.

Lienert B., 1994, HYPOCENTER 3.2 Manual. Honolulu: HIGP.

Lienert B., Berg E., Frazer L.N., 1986, HYPOCENTER: An earthquake location method using centered, scaled and adaptively damped least squares. *Bull. Seis. Soc. Am.*, 76, 771-783.

Lienert B., Havskov J., 1995, Computer program for locating earthquakes both locally and globally. *Seis. Res. Lett.*, 66, 26-36.

Lomnitz C., 2006, Three Theorems of Earthquake Location. *Bull. Seis. Soc. Am*., 96, 306-312. Doi:10.1785/0120050039.

López Ramos E., 1983, Geología de México. (3rd ed.). Mexico, D.F., Editorial México.

Macías J., Siebe C., 2005, Popocatépetl crater fillled to the brim: significance for hazard evaluation. *J. Volc. Geoth. Res.*, 141, 327-330.

Meritano-Arenas J.D., Rosales-Gómez J., Conde-Asiain A., 1998, Carta Geológica y Carta Morfoestructural del Popocatépetl. Consejo de Recursos Minerales Ministry of Comerce and Industry (Secretaría de Comercio y Fomento Industrial) (SECOFI).

Minakami T., 1974, Seismology of Volcanoes in Japan: Physical Volcanology. Amsterdam: Elsevier.

Mullineaux D., Crandell D., 1981, The 1980 eruptions of mount St. Helens, Washington. chapter The Eruptive History of Mount St. Helens. (p. 844). U.S. Geological Survey Professional Paper 1250.

Nava A.F., 2010, A Local Earthquake Location Method, based on time difference fitting

through Genetic Search, for Tectonic and Volcanological Applications. Comunicaciones Academicas (Open-file report) CICESE, 8, 195-209.

Novelo-Casanova D.A., Valdés-González C., Ramírez-Olvera G., 2007, A numerical model for the mechanical behavior of Popocatépetl volcano (Central Mexico). *Phys. Earth Plan. Int.*, 162, 99-110. Doi:10.1016/j.jvolgeores.2007.03.001.

Poupinet G., Ellsworth W., Fréchet J., 1984, Monitoring velocity variations in the crust using earthquake doublets: An application to the Calaveras fault, California. *J. Phys. Earth*, 89, 719-731.

Ramírez-Olvera, G., 2003, Mallado tridimensional para elemento finito del Volcán Popocatépetl, correlacionado con la sismicidad. Bachelor's thesis Universidad Autónoma Nacional de Mexico.

Roberge J., Delgado-Granados H., Wallace P.J., 2007, Determination of the degassing depth at Popocatépetl volcano (Mexico) using data from olivine-hosted melt inclusions. In American Geophysical Union, Fall Meeting 2007. San Francisco. Abstract No. V42B-05.

Rubin A., Gillard D., Got J.-L., 1998, A re-examination of seismicity associated with the January 1983 dike intrusion at Kilauea volcano, Hawaii. *J. Geoph. Res.*, 103, 10,003-10,015.

Shapiro N.M., Campillo M., Paul A., Singh S., Jongmans D., Sanchez-Sesma F., 1997, Surface wave propagation across the Mexican volcanic belt and the origin of the long period seismic wave amplication in the Valley of Mexico. *Geophy. J. Int.*, 128, 151-166.

Shearer P., 1997, Improving local earthquake locations using the l1 norm and waveform cross-correlation: Application to the Whittier Narrows, California, aftershock sequence. *J. Geophy. Res.*, 102, 8,269-8,283.

Siebe C., Abrams M., Macías J.L., Obenholzner J., 1996, Repeated volcanic disaster in prehispanic time at Popocatépetl, Central Mexico: Past key to the future? *Geology*, 24, 399-402.

Siebe C., Macías J., 1997, Volcanic hazards in the Mexico City metropolitan area from eruptions at Popocatépetl, Nevado de Toluca, and Jocotitlán stratovolcanoes and monogenetic scoria cones in the Sierra de Chichinautzin volcanic eld. *Field Trip Guidebook, Geol. Soc. Am.*, 1, 77.

Slunga R., Roegnvaldsson S., Boedvarsson R., 1995, Absolute and relative locations of similar events with application to microearthquakes in southern Iceland. *Geophy. J. Int.*, 123, 409-419.

Straub S.M., Martín-Del-Pozzo A.L., 2001, The significance of phenocryst diversity in tephra from recent eruptions of Popocatépetl Stratovolcano (central Mexico): Contributions to Mineralogy and Petrology. *Geophy. J. Int.*, 140, 487-510.

Valdés C., González G., Arcieniega A., Guzmán M., Nava E., Gutiérrez C., Santoyo M., 1995, Volcan Popocatépetl, Estudios realizados durante la crisis de 1994-1995. chapter Sismicidad del Volcán Popocatépetl a partir del 21 de Diciembre de 1994 al 30 de Marzo de 1995. pp. 129-138). México, D.F.: CENAPRED-UNAM (ed.).

Valdés C.M., Mooney W., Singh S., Meyer R., Lomnitz C., Luetgert J.H., Hesley B., Lewis B., Mena M., 1986, Crustal structure of Oaxaca, Mexico from seismic refraction measurements. *Bull. Seis. Soc. Am.*, 76, 547-564.

Valdés-Gonzalez C.M., Comité C.d.V.P., 1994, P-wave 1D velocity model, Popocatépetl, Mexico.

Waldhauser F., 2001, HypoDD - A program to compute Double-Difference hypocenter locations. U.S. Geol. *Survey Open File Report*, 1-113, 1-25.

Waldhauser F., Ellsworth W.L., 2000, Double difference earthquake location algorithm: method and application to the Northern Hayward fault, California. *Bull. Seis. Soc. Am.*, 90, 1,353-1,368.

Wolfe C.J., 2002, On the mathematics of using difference operators to relocate earthquakes. *Bull. Seis. Soc. Am.*, 92, 2,879-2,892.

Wright R., De la Cruz-Reyna S., Harris A., Flynn L., Gómez-Palacios J., 2002, Infrared satellite monitoring at Popocatépetl: explosions, exhalations, and cycle of dome growth. *J. Geophy. Res.*, 107 B8, 1,029-1,045.